Magnetoviscous model fluids

2003 J. Phys.: Condens. Matter 15 S1403

(http://iopscience.iop.org/0953-8984/15/15/307)

INSTITUTE OF PHYSICS PUBLISHING JOURNAL OF PHYSICS: CONDENSED MATTER

J. Phys.: Condens. Matter **15** (2003) S1403–S1423 PII: S0953-8984(03)54527-1

Magnetoviscous model fluids

Martin Kröger[1,2], **Patrick Ilg**[1] **and Siegfried Hess**[1]

[1] Institut für Theoretische Physik, Fakultät II, Technische Universität Berlin, Hardenbergstrasse 36, D-10623 Berlin, Germany
[2] Polymer Physics, Material Sciences, ETH Zürich, ML H18, 8092 Zürich, Switzerland

E-mail: mkroeger@mat.ethz.ch

Received 9 October 2002
Published 7 April 2003
Online at stacks.iop.org/JPhysCM/15/S1403

Abstract

We review, apply and compare diverse approaches to the theoretical understanding of the dynamical and rheological behaviour of ferrofluids and magnetorheological (MR) fluids subject to external magnetic and flow fields. Simple models are introduced which are directly solvable by nonequilibrium Brownian or molecular dynamics computer simulation. In particular, the numerical results for ferrofluids quantify the domain of validity of uniaxial alignment of magnetic moments (in and) out of equilibrium. A Fokker–Planck equation for the dynamics of the magnetic moments—corresponding to the Brownian dynamics approach—and its implications are analysed under this approximation. The basic approach considers the effect of external fields on the dynamics of ellipsoid shaped permanent ferromagnetic domains (aggregates), whose size should depend on the strength of flow and magnetic field, the magnetic interaction parameter and concentration (or packing fraction). Results from analytic calculations and from simulation are summarized for the anisotropy of the viscosity. In order to study the effect of flow on the anisotropic viscosities and shear-induced structures of MR fluids and ferrofluids subject to a strong external magnetic field, a simple model of perfectly oriented particles is considered.

1. Introduction

Magnetorheological (MR) fluids contain particles that are paramagnetic, i.e. become magnetized on application of a magnetic field. Ferrofluids, on the other hand, contain colloidal particles with a permanent ferromagnetic core. Both types of fluids, usually composed of spherical particles, show an anisotropic flow behaviour in the presence of a magnetic field. Ferrofluids, however, show a flow-induced anisotropy even in the absence of an external magnetic field due to their ability to form magnetic aggregates or superstructures in the field-free state. These fluids are usually stabilized against agglomeration by coating particles with

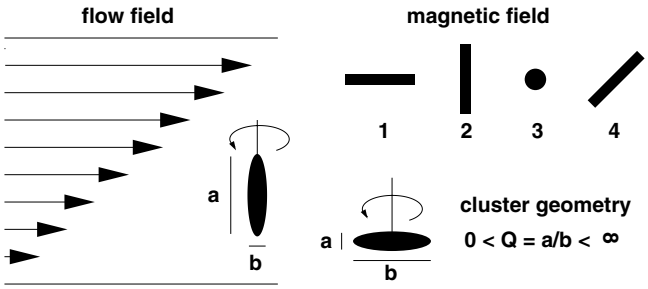

Figure 1. Schematic drawing depicting the geometry of the physical situation. For the measurement of the Miesowicz viscosities $\eta_{1,2,3}$ and the viscosity η_4 the magnetization induced by the external magnetic field has to point in flow (1), flow gradient (2) and vorticity (3) directions. The ellipsoids of revolution considered within the FP approach are characterized by a single shape factor $0 < Q < \infty$, where $Q > 1$ and $Q < 1$ for rod-like and disc-like aggregates, respectively.

long-chain molecules (sterically) or decorating them with charged groups (electrostatically). Particles interact with each other by the long-range anisotropic dipole–dipole potential as well as the short-range symmetric potentials, such as the steric repulsion, the electrostatic repulsion and the van der Waals attraction. The rheology of ferrofluids can be understood in terms of the concurrent orienting mechanism stemming from flow and magnetic field, where the coupling to the flow field becomes increasingly important with the formation of aggregates, see figure 1. Dipolar interactions, present in both types of fluids, influence the pair correlation function. Its characteristic anisotropy and shear-induced distortion are directly related to the rheological properties. The magnetic relaxation is dominated by two distinct mechanisms: the Néel relaxation describes the reorientation of the magnetic core relative to the particle's surface which is in contact with the carrier fluid. This is in contrast to the Brownian process, where relaxation takes place via rotation of the whole particle relative to the fluid. For sufficiently large particles the Brownian mechanism prevails. This is the case considered in sections 3 and 4, while section 5 deals with (fully) oriented magnetic moments.

Phenomenologically, the anisotropy of the viscosity can be characterized by the same set of viscosity coefficients [1] as used for uniaxial nematic liquid crystals in the presence of an orienting (electric or magnetic) field [2–7]. This is not obvious, since the magnetic field introduces a new direction, but will be clarified below for the case of uniaxial symmetry, where this statement applies. Moreover, the microscopic mechanisms leading to the anisotropic viscous behaviour are rather different in these systems. Even for ferrofluids, the microscopic mechanisms responsible for the peculiar flow behaviour of dilute solutions, where the magnetic field-induced change of the viscosity is linear with the concentration of ferrofluid particles, are different from that of more concentrated solutions. There the direct anisotropic interaction between the ferrofluid particles becomes the dominating mechanism. Theoretical descriptions applicable to ferrofluids are given in [8–11]. In [11] the linear and nonlinear rheological behaviour of dilute ferrofluids is determined from an underlying kinetic model and the dependence of the viscosity coefficient on the scalar orientational order parameters is obtained. In the case of uniaxial symmetry, the antisymmetric contribution to the hydrodynamic stress tensor is of the same form as in the classical Ericksen–Leslie theory of uniaxial nematic liquid crystals and the linear magnetoviscosity is found to coincide with earlier results obtained by the effective field method [11–13]. While the assumption of uniaxial symmetry is fulfilled exactly in the limit of strong vorticity and weak magnetic field, the exact result for the linear magnetoviscosity shows corrections due to contributions from biaxial symmetry.

A number of theoretical models allow the evaluation of the equilibrium magnetization of ferrofluids [14–21]. Among them, the mean-spherical model [16, 17], the thermodynamic perturbation model [18] and the modified variant of the effective field model [19] have been shown to give good results for the magnetic properties of ferrofluids with low or moderate concentrations of magnetic particles (up to 10–12%). For ferrofluids of higher concentration, larger particle size or at low temperature, these descriptions become insufficient [20, 22]. In [23] the kinetic model of non-interacting magnetic dipoles [8] is extended to incorporate the effect of weak dipolar interactions. The extended model shows similarities to the dynamic mean-field theory of liquid crystalline polymers proposed in [24]. In qualitative agreement with experimental results, this model predicts an enhanced equilibrium magnetization, the existence of an anisotropy of the viscosity tensor characterized by five independent viscosity coefficients, normal stress differences and an improved concentration dependence of the viscosity coefficients.

To highlight the phenomena associated with the case of more concentrated MR suspensions, a simple model of perfectly aligned magnetic moments is also reviewed here. It has previously been used to treat equilibrium [25] and nonequilibrium properties [25–30] of dense ferrofluids and MR fluids, where a yield stress can occur in the presence of a magnetic field, and agglomerates, or chains, are formed at sufficiently large magnetic interaction strength. Chains break down under shear. As a consequence, one observes a strong shear thinning. This not only occurs in MR fluids, but also in ferrofluids composed of particles with permanent magnetic dipole moments, even without an applied field. Methods developed for the study of flow properties of 'living polymers' [31–33] and actin filaments [34] can be applied to ferrofluids. In order to study the effect of clustering on the rheological properties, a phenomenon first discussed by Rosensweig [35], implications of a Fokker–Planck (FP) equation for ellipsoidal ferromagnetic aggregates [13] will be discussed below.

This paper is organized as follows. Section 2 contains remarks about isotropic and anisotropic viscosities, their measurement, their qualitative behaviours and their relevance for the rheological description of ferrofluids with special emphasis on the case of shear flow. Section 3 starts from a FP equation for dilute suspensions of ferrofluids subject to external fields. Here, expressions for the viscosities in terms of order parameters are obtained, underpinning the qualitative discussion of section 2. Results for the FP extension to the case of ellipsoidal aggregates are reported in section 3, and the predictions are further compared with a numerical solution of the FP equation, i.e. with results from nonequilibrium Brownian dynamics (NEBD) computer simulations in section 4. Next in section 5, we present nonequilibrium molecular dynamics (NEMD) results for a simple many-particle model of MR fluids which does not take into account the effect of orientational degrees of freedom of paramagnetic particles. The model of perfectly oriented magnetic moments (all order parameters become unity) already provides us with a 'realistic scenario' for the dependence of anisotropic viscosities and the related structural behaviour on the magnetic interaction parameter and shear rate, see section 6. It also provides a microscopically based measurement of the size of agglomerates and allows us to test the effect of concentration on the rheological and structural properties, and to quantify the applicability of the results obtained from the FP approach.

2. Anisotropic viscosities

General remarks, isotropic liquids

The viscosity characterizes the transport of linear momentum through a fluid. For a simple shear flow geometry $\boldsymbol{v} = (v_x(y), 0, 0)$ with flow (x), gradient (y) and vorticity (z) direction,

the (shear) viscosity is defined as the ratio of the component p_{yx} of the pressure (negative stress) tensor and shear rate $\dot{\gamma} = \partial v_x/\partial y$ through $p_{yx} = -\eta\dot{\gamma}$. For a more general geometry, a tensorial description is needed. The pressure tensor $\boldsymbol{P}$ occurring in the local conservation equation for the linear momentum $\rho\,\mathrm{d}\boldsymbol{v}/\mathrm{d}t + \boldsymbol{\nabla}\cdot\boldsymbol{P} = \boldsymbol{0}$ is the sum of its equilibrium value $P_{\mathrm{eq}}\mathbf{1}$, where $\mathbf{1}$ is the unit tensor, and of the friction pressure tensor $\boldsymbol{p}$: $\boldsymbol{P} = P_{\mathrm{eq}}\mathbf{1} + \boldsymbol{p}$. Like any second rank tensor, the latter quantity can be decomposed into its isotropic, antisymmetric and symmetric traceless parts:

$$\boldsymbol{p} = p\mathbf{1} + \tfrac{1}{2}\boldsymbol{\epsilon}\cdot\boldsymbol{p}^{\mathrm{a}} + \overline{\boldsymbol{p}}\,, \tag{1}$$

where $p = \mathrm{Tr}\boldsymbol{p}/3$ is one-third of the trace of the friction pressure tensor. The antisymmetric part of the tensor involves the pseudo-vector $\boldsymbol{p}^{\mathrm{a}} = -\boldsymbol{\epsilon}\colon\boldsymbol{p}$, where the quantity $\boldsymbol{\epsilon}$ is the totally antisymmetric isotropic third rank (Levi–Civita) tensor. The symbol $\overline{\ldots}$ indicates the symmetric traceless part of a tensor, in particular: $\overline{\boldsymbol{p}} = (\boldsymbol{p} + \boldsymbol{p}^{\mathrm{T}})/2 - (\mathrm{Tr}\boldsymbol{p})\mathbf{1}/3$. The velocity gradient tensor can be decomposed, in analogy to (1), $\boldsymbol{\nabla}\boldsymbol{v} = (\boldsymbol{\nabla}\cdot\boldsymbol{v})\mathbf{1}/3 + \boldsymbol{\epsilon}\cdot\boldsymbol{\omega} + \boldsymbol{\gamma}$. The divergence $\boldsymbol{\nabla}\cdot\boldsymbol{v}$ of the velocity field vanishes for a volume conserving flow of a practically incompressible fluid. The quantity $\boldsymbol{\omega} = (\boldsymbol{\nabla}\times\boldsymbol{v})/2$ is the vorticity of the flow field. The symmetric traceless part of the velocity gradient tensor, $\boldsymbol{\gamma} \equiv \overline{\boldsymbol{\nabla}\boldsymbol{v}} = (\boldsymbol{\nabla}\boldsymbol{v} + (\boldsymbol{\nabla}\boldsymbol{v})^{\mathrm{T}})/2 - (\boldsymbol{\nabla}\cdot\boldsymbol{v})\mathbf{1}/3$ is referred to as the deformation rate tensor.

The antisymmetric part of the pressure tensor is identically zero for substances composed of point particles with isotropic interaction. Under most practical circumstances, in particular for stationary situations and in the absence of external fields, the antisymmetric part of the pressure tensor becomes zero for molecular fluids in the isotropic phase. As a consequence, the quantity $\boldsymbol{p}^{\mathrm{a}}$ vanishes. Then, in the linear flow regime, two viscosity coefficients, namely the above-mentioned shear viscosity η and the bulk or volume viscosity η_{V}, suffice to characterize the viscous behaviour of an isotropic fluid: $\overline{\boldsymbol{p}} = -2\eta\,\overline{\boldsymbol{\nabla}\boldsymbol{v}}$, $p = -\eta_{\mathrm{V}}\boldsymbol{\nabla}\cdot\boldsymbol{v}$. Note again that, for an incompressible fluid, or for a volume conserving flow, one has $\boldsymbol{\nabla}\cdot\boldsymbol{v} = 0$. In the following we will focus on results for incompressible fluids.

The viscosity coefficients of nematic liquid crystals and ferrofluids

For a nematic fluid with the director field $\boldsymbol{n} = \boldsymbol{n}(t, \boldsymbol{r})$, and with the corotational time derivative of the director denoted by $\boldsymbol{N} \equiv \dot{\boldsymbol{n}} - \boldsymbol{\omega}\times\boldsymbol{n}$ the ansatz [1, 5]

$$\begin{aligned}-\boldsymbol{p} = {}& \alpha_1\boldsymbol{\gamma}\colon\boldsymbol{nnnn} + \alpha_2\boldsymbol{nN} + \alpha_3\boldsymbol{Nn} + \alpha_4\boldsymbol{\gamma} + \alpha_5\boldsymbol{nn}\cdot\boldsymbol{\gamma} + \alpha_6\boldsymbol{\gamma}\cdot\boldsymbol{nn} \\ & + \zeta_1\boldsymbol{nn}\colon\boldsymbol{\gamma}\mathbf{1} + \zeta_2(\boldsymbol{\nabla}\cdot\mathbf{v})\boldsymbol{nn} + \zeta_3(\boldsymbol{\nabla}\cdot\mathbf{v})\mathbf{1}\end{aligned} \tag{2}$$

is used to describe the viscosity. This relation is linear in the velocity gradient and in the corotational derivative of the director. Furthermore, it is invariant under the replacement of $\boldsymbol{n}$ by $-\boldsymbol{n}$, as it should be. The Leslie coefficients $\alpha_1, \ldots, \alpha_6$ and the coefficients ζ_1, ζ_2, ζ_3 have the dimension of a viscosity.

Decomposition of the pressure tensor and the velocity gradient tensor into their isotropic, antisymmetric and symmetric traceless parts leads to the linear constitutive laws [1]

$$\begin{aligned}\overline{\boldsymbol{p}} = {}& -2\eta\boldsymbol{\gamma} - 2\tilde{\eta}_1\,\overline{\overline{\boldsymbol{nn}}\cdot\boldsymbol{\gamma}} - 2\tilde{\eta}_2\,\overline{\boldsymbol{nN}} \\ & - 2\tilde{\eta}_3\,\overline{\boldsymbol{nn}}\,\boldsymbol{nn}\colon\boldsymbol{\gamma} - \zeta_2\,\overline{\boldsymbol{nn}}\,(\boldsymbol{\nabla}\cdot\boldsymbol{v}),\end{aligned} \tag{3}$$

$$\boldsymbol{p}^{\mathrm{a}} = \boldsymbol{\epsilon}\colon(\gamma_1\boldsymbol{nN} + \gamma_2\,\overline{\boldsymbol{nn}}\cdot\boldsymbol{\gamma}), \tag{4}$$

$$p = -\eta_{\mathrm{V}}\boldsymbol{\nabla}\cdot\boldsymbol{v} - \kappa\boldsymbol{\gamma}\colon\boldsymbol{nn}. \tag{5}$$

The viscosity coefficients used in equations (3)–(5) are related to those of equation (2) by $2\eta = \alpha_4 + (\alpha_5 + \alpha_6)/3$, $2\tilde{\eta}_1 = (\alpha_5 + \alpha_6)$, $2\tilde{\eta}_2 = (\alpha_2 + \alpha_3)$, $2\tilde{\eta}_3 = \alpha_1$, $\gamma_1 = \alpha_3 - \alpha_2$, $\gamma_2 = \alpha_6 - \alpha_5$, $\eta_V = \zeta_2/3 + \zeta_3$, and $\kappa = \zeta_1 + (\alpha_1 + \alpha_5 + \alpha_6)/3$. The dyadic $\overline{\boldsymbol{nn}}$ stems from the second rank alignment tensor. The coefficients linking second with first rank tensors, and second rank tensors with scalars (rank 0) obey Onsager symmetry relations. These are $2\tilde{\eta}_2 = \gamma_2, \zeta_2 = \kappa$, where the first of these relations is equivalent to the Onsager–Parodi relation [4] $\alpha_2 + \alpha_3 = \alpha_6 - \alpha_5$. Due to the symmetry relations, only 7 of the 9 viscosity coefficients are linearly independent. In an isotropic fluid all coefficients vanish except for the shear viscosity $\eta = \frac{1}{2}\alpha_4$ and the bulk viscosity $\eta_V = \zeta_3$. Positive entropy production requires $\eta > 0, \eta_V > 0, \gamma_1 > 0$ but $\tilde{\eta}_1, \tilde{\eta}_2, \tilde{\eta}_3$ and γ_2 may have either sign. One standard set of viscosity coefficients are the $\alpha_1, \ldots, \alpha_6$ of equation (2). The coefficients occurring in the ansatz (3)–(5) can be preferable in connection with theoretical considerations. In experiments and in NEMD simulations, linear combinations of the 'basic' viscosity coefficients are measured and calculated. Some examples are mentioned next.

In a plane Couette or a plane Poiseuille flow with the velocity in the x direction and its gradient in the y direction one has $\boldsymbol{\nabla v} = \dot{\gamma}\mathrm{e}^y\mathrm{e}^x, \boldsymbol{\omega} = -\dot{\gamma}\mathrm{e}^z/2$, with the shear rate $\dot{\gamma} = \partial v_x/\partial y$, and $\mathrm{e}^{x,y,z}$ are unit vectors parallel to the x-, y-, z-coordinate axes. The Miesowicz viscosities $\eta_i, i = 1, 2, 3$ are defined as the ratio of the negative yx component of the pressure tensor and the shear rate $\dot{\gamma}$: $p_{yx}^{(i)} = -\eta_i\dot{\gamma}$. The label $i = 1, 2, 3$ refers to the cases where the director $\boldsymbol{n}$ is parallel to the x, y and z axis, respectively. The orienting (magnetic) field has to be strong enough to overcome the flow induced orientation. A fourth coefficient η_4 with $\boldsymbol{n}$ parallel to the bisector between the x and y axes is needed to characterize the shear viscosity completely. Instead of η_4, the Helfrich viscosity coefficient $\eta_{12} = 4\eta_4 - 2(\eta_1 + \eta_2)$ is used in addition to the Miesowicz coefficients. The 'rotational' viscosity γ_1 can be measured via the torque exerted on a nematic liquid crystal in the presence of a rotating magnetic field: the Tsvetkov effect [36–38]. The four effective viscosities measurable in a flow experiment are related to the viscosity coefficients of equation (2) and equations (3)–(5) by

$$\begin{aligned}
\eta_1 &= \tfrac{1}{2}(\alpha_4 + \alpha_6 + \alpha_3) = \eta + \tfrac{1}{6}\tilde{\eta}_1 + \tfrac{1}{2}\tilde{\eta}_2 + \tfrac{1}{4}(\gamma_1 + \gamma_2),\\
\eta_2 &= \tfrac{1}{2}(\alpha_4 + \alpha_5 - \alpha_2) = \eta + \tfrac{1}{6}\tilde{\eta}_1 - \tfrac{1}{2}\tilde{\eta}_2 + \tfrac{1}{4}(\gamma_1 - \gamma_2),\\
\eta_3 &= \tfrac{1}{2}\alpha_4 = \eta - \tfrac{1}{3}\tilde{\eta}_1, \qquad \eta_{12} = 4\eta_4 - 2(\eta_1 + \eta_2) = \alpha_1 = 2\tilde{\eta}_3.
\end{aligned} \tag{6}$$

The antisymmetric part of the pressure tensor contributes to η_1 and η_2 but not to η_3 and η_{12}. Notice that $\eta_1 + \eta_2 + \eta_3 = 3\eta + \gamma_1/2$, $\eta_1 - \eta_2 = 2\tilde{\eta}_2 = \gamma_2$, $\eta_1 + \eta_2 - 2\eta_3 = \tilde{\eta}_1$. By symmetry arguments, the same set of viscosity coefficients can be used for ferrofluids in the presence of a magnetic field. The director has to be replaced by a unit vector parallel to the local magnetization which, for strong applied fields, is parallel to the direction of the external field.

The following considerations are limited to the case of either zero or a 'strong' field. Theories appropriate for dilute solutions, which just take into account that the magnetic field affects or hinders the rotation of a particle and associate the magneto-viscous effect solely with the antisymmetric part of the pressure tensor, imply that γ_1 is nonzero and depends on the field strength and the shear rate. In that case, however, one has $\tilde{\eta}_1 = 0$, $\tilde{\eta}_2 = 0$, and consequently $\eta_1 - \eta_2 = \gamma_2 = 0$, as well as $\eta_{12} = 0$. Then the McTague [39] viscosity coefficients $\eta_\parallel = \eta_1$ and $\eta_\perp = (\eta_2 + \eta_3)/2$ become equal to $\eta + \gamma_1/4$ and $\eta + \gamma_1/8$, respectively. The anisotropy observed for the ferrofluids of [39] are indeed of that type. In general, the anisotropy found in more concentrated ferrofluids is more complex and it is expected that all viscosity coefficients needed by symmetry considerations will be nonzero. So far, there is no precise experimental data available for the complete set of coefficients. However, experimentally observed effects due to the influence of magnetic fields on the rotation of single magnetic

nanoparticles, as well as cooperative phenomena and their importance for viscous effects in ferrofluids, have been reviewed in [40–42]. In particular, a change of field-induced increase of viscosity due to variation of the shear rate applied to the fluid has been reported in [43], see also [44]. The transition area between elastic and viscous behaviour for a conventional ER fluid and a state-of-the-art MR fluid through the use of oscillatory rheometry techniques has been investigated [45]. More recently, neutron scattering [46] and microgravity [47] have been applied to resolve structural effects and flow profiles in MR fluids. Inhomogeneities in particle concentration have been considered in order to explain an enormous increase of yield stresses of MR and electro-rheological (ER) suspensions subjected to magnetic or electric fields in [48–51].

Next, we will derive explicit expressions for the anisotropic viscosities from a FP equation.

3. Fokker–Planck equation for ferrofluids

Consider an ensemble of n non-interacting, identical, rigid, ferromagnetic ellipsoids of revolution (axis ratio Q, shape factor $B \equiv (Q^2-1)/(Q^2+1)$) per volume. Spherical particles constitute a special case ($B = 0$), while the ellipsoidal shape accounts for the formation of effectively ellipsoidal clusters. We assume the system to be spatially homogeneous, so that the state is described by the probability distribution function $f(\boldsymbol{u}; t)$ of an ellipsoid being oriented in the direction of the unit vector $\boldsymbol{u}$ at time t. Furthermore, it is assumed that the symmetry axis coincides with the direction of magnetization of the particles, $\boldsymbol{\mu} = \mu\boldsymbol{u}$. The motion of a single ellipsoid is influenced by rotational diffusion, motion due to an external potential V and the hydrodynamic drag caused by velocity field $\boldsymbol{v}$. The dynamics is conveniently described by the kinetic equation [24, 52, 53]

$$\partial_t f = -\boldsymbol{\mathcal{L}} \cdot (\boldsymbol{\omega} + B\boldsymbol{u} \times \boldsymbol{\gamma} \cdot \boldsymbol{u}) f + \tfrac{1}{2}\tau^{-1} \boldsymbol{\mathcal{L}} \cdot f \boldsymbol{\mathcal{L}}[\ln f + V/k_\mathrm{B}T], \tag{7}$$

where the potential V for a magnetic moment $\boldsymbol{\mu} = \mu\boldsymbol{u}$ in the local magnetic field $\boldsymbol{H}$ is given by $-\beta V = \beta\mu\boldsymbol{H} \cdot \boldsymbol{u} = \boldsymbol{h} \cdot \boldsymbol{u}$, with $\beta \equiv 1/(k_\mathrm{B}T)$. Hereby the dimensionless magnetic field $\boldsymbol{h} = \mu\boldsymbol{H}/k_\mathrm{B}T$ and its amplitude h (Langevin parameter) are introduced, where $\boldsymbol{\mathcal{L}} = \boldsymbol{u} \times \nabla_u$ is the rotational operator with ∇_u being the gradient on the unit sphere. For spheres, $B = 0$, equation (7) reduces to the kinetic equation for dilute ferrofluids given in [11, 12, 53]. The relaxation time τ of the ellipsoidal unit is related to its rotary diffusion coefficient D_r and its rotary friction coefficient $\zeta_\mathrm{rot} = 6V_p\eta_\mathrm{s}e_Q$ via $D_r^{-1} = 2\tau = \zeta_\mathrm{rot}/k_\mathrm{B}T$ [13], where η_s is the shear viscosity of the Newtonian solvent, e_Q is the shape factor given below[3] and V_p denotes the volume of a single ellipsoid. The magnetization (density) $\boldsymbol{M}$ is obtained from the first moment of the distribution function as $\boldsymbol{M} = n\mu\langle\boldsymbol{u}\rangle$. The FP approach (7) neglects magnetization inertia effects.

3.1. Pressure tensor and magnetization

The hydrodynamic pressure tensor $\boldsymbol{p}$ for an incompressible dilute suspension of rigid ellipsoidal particles is, according to [52–54],

$$\overline{\boldsymbol{p}} = -2\eta_\mathrm{s}(1 + 5\phi Q_1)\boldsymbol{\gamma} + \overline{\boldsymbol{p}}^{\,\mathrm{pot}} - 10\eta_\mathrm{s}\phi\{(2Q_3 - BQ_0)\,\overline{\boldsymbol{\gamma} \cdot \langle\boldsymbol{uu}\rangle} - (Q_{23} - 2BQ_0)\,\overline{\boldsymbol{\gamma}\colon\langle\boldsymbol{uuuu}\rangle}\}, \tag{8}$$

$$\boldsymbol{p}^\mathrm{a} = -n\langle\boldsymbol{\mathcal{L}}V\rangle, \tag{9}$$

[3] For slightly deformed spheres with axis ratio $Q = 1 + \epsilon$, $\epsilon \ll 1$ one finds $B = \epsilon$ and for the geometric coefficients Q_i and e_Q up to $\mathcal{O}(\epsilon^2)$: $Q_0 = 3\epsilon/5 - 9\epsilon^2/50$, $Q_1 = 1/2 - \epsilon/7 + 47\epsilon^2/294$, $Q_2 = -2\epsilon/7 + \epsilon^2/21$, $Q_3 = 3\epsilon/14 - 13\epsilon^2/2940$. $Q_{23} \equiv 3Q_2 + 4Q_3$, $Q_{32} \equiv Q_3 - Q_2$, $e_Q \equiv (5Q_0)/(3B) = 1 + \epsilon/5 + 179\epsilon^2/350$. More explicit expressions for these coefficients for all Q are given in [13].

where η_s is the shear viscosity of the Newtonian solvent and ϕ stands for the packing fraction. The geometric coefficients $Q_i = Q_i(Q)$ are defined in [11, 13] (and also see footnote 3) and the anisotropic potential contribution is given by

$$\overline{\boldsymbol{p}}^{\,\mathrm{pot}} = -nk_\mathrm{B}TB\langle\,\overline{\boldsymbol{u}\nabla_{\boldsymbol{u}}}\,(\ln f + V/k_\mathrm{B}T)\rangle. \tag{10}$$

Here and below, $\langle\cdot\cdot\rangle$ denotes an average with respect to the distribution function f, where the integration is performed over the three-dimensional unit sphere. The antisymmetric part of the stress tensor is of the form also used in [52, 55, 56, 58–73], while an additional antisymmetric stress has been proposed in [57]. Inserting the potential V into equations (9) and (10) one obtains

$$\overline{\boldsymbol{p}}^{\,\mathrm{pot}} = -nk_\mathrm{B}TB(3\langle\,\overline{\boldsymbol{uu}}\,\rangle - \overline{\langle\boldsymbol{u}\rangle\boldsymbol{h}} + \overline{\langle\boldsymbol{uuu}\rangle\cdot\boldsymbol{h}}\,), \tag{11}$$

$$\boldsymbol{p}^\mathrm{a} = nk_\mathrm{B}T\langle\boldsymbol{u}\rangle\times\boldsymbol{h} = \boldsymbol{M}\times\boldsymbol{H}, \tag{12}$$

where equation (11) is obtained from equation (10) by an integration by parts, and the above definitions for the dimensionless magnetic field $\boldsymbol{h} = \mu\boldsymbol{H}/k_\mathrm{B}T$ and the magnetization $\boldsymbol{M} = n\mu\langle\boldsymbol{u}\rangle$ are used to rewrite the pseudo-vector $\boldsymbol{p}^\mathrm{a}$. In the absence of a flow field, equation (7) yields a unique equilibrium state f_eq. The approach to equilibrium is monitored by the dimensionless free energy functional per particle, $F[f] = \int_{S_2} \mathrm{d}^2u\, f(\boldsymbol{u})\ln(f(\boldsymbol{u})/f_\mathrm{eq}(\boldsymbol{u}))$. The equilibrium magnetization directly obtained from the equilibrium distribution of the FP equation is $\boldsymbol{M}_\mathrm{eq} = n\mu\,\langle\boldsymbol{u}\rangle_\mathrm{eq} = n\mu L(h)\boldsymbol{h}/h$, where $L(x) \equiv \coth(x) - 1/x$ is the Langevin function. This equilibrium magnetization is the classical result for a system of non-interacting magnetic dipoles. The stationary solution to equation (7) in the case of steady potential flow, $\boldsymbol{\omega} \equiv \boldsymbol{0}$, can also be found explicitly [13]. From the kinetic equation (7), the dynamics of the kth moment $\langle u_{\alpha_1}\cdots u_{\alpha_k}\rangle$ is obtained by multiplying the FP equation by $\boldsymbol{uu}\ldots$ and subsequent integration over the unit sphere. The equation for the first moment, $k = 1$, i.e. the magnetization $\boldsymbol{M}$, is therefore

$$\partial_t\langle\boldsymbol{u}\rangle = \boldsymbol{\omega}\times\langle\boldsymbol{u}\rangle + B\langle(\boldsymbol{1}-\boldsymbol{uu})\boldsymbol{u}\rangle{:}\,\boldsymbol{\gamma} - \frac{1}{\tau}\langle\boldsymbol{u}\rangle + \frac{1}{2\tau}(\boldsymbol{1}-\langle\boldsymbol{uu}\rangle)\cdot\boldsymbol{h}. \tag{13}$$

The one for the second moment is worked out in [13]. Using these equations of change, the explicit contribution of the potential V to the full stress tensor can be eliminated [52]. In particular, one obtains for the antisymmetric part (12), upon inserting the following result [13]:

$$\boldsymbol{h} = \tau\boldsymbol{\Pi}^{-1}\cdot(\partial_t\langle\boldsymbol{u}\rangle - \boldsymbol{\omega}\times\langle\boldsymbol{u}\rangle - B[\boldsymbol{\gamma}\cdot\langle\boldsymbol{u}\rangle - \langle\boldsymbol{uuu}\rangle{:}\,\boldsymbol{\gamma}] + \tau^{-1}\langle\boldsymbol{u}\rangle), \tag{14}$$

where $\boldsymbol{\Pi}^{-1}$ denotes the inverse of the matrix $\boldsymbol{\Pi} \equiv (\boldsymbol{1} - \langle\boldsymbol{uu}\rangle)$, an expression for $\boldsymbol{p}^\mathrm{a}$ in terms of the moments alone. In the absence of potential forces and for $\dot\gamma \to 0$, the steady state pressure tensor $\boldsymbol{p}$ reduces to $\boldsymbol{p} = -2\eta_0\boldsymbol{\gamma}$, with the zero-shear viscosity of a dilute suspension of magnetically neutral ellipsoidal particles with axis ratio Q and shape coefficients Q_i [13] (and also see footnote 3) as follows: $\eta_0 = \eta_s\{1+\phi(5Q_1+(2Q_3-Q_2))\}$. Therefore Einstein's formula $\eta_0 = (1 + 5\phi/2)\eta_s$ is recovered from this expression for spherical particles (see footnote 3). For later use we introduce the extra viscosity

$$\eta_0^\phi \equiv \eta_0 - \eta_s = \phi(5Q_1 + (2Q_3 - Q_2))\eta_s, \tag{15}$$

which arises due to the presence of ellipsoidal aggregates at concentration ϕ. Due to the hydrodynamic drag and the magnetic field, the equation for the moment of order k couple to moments of order $k \pm 1$ and $k \pm 2$ ($k \geqslant 0$). Therefore, a finite set of closed equations for the macroscopic magnetization and the macroscopic pressure tensor $\boldsymbol{p}$ cannot in general be derived from the kinetic model unless some approximations are invoked.

3.2. Pressure tensor and viscosities in terms of order parameters

In order to obtain more explicit expressions for the stress tensor and the viscosity coefficients, we now consider the class of distribution functions, which are uniaxially symmetric with respect to the unit vector $\boldsymbol{n}$. Therefore f has the representation $4\pi f_{\text{uni}}(\boldsymbol{u}\cdot\boldsymbol{n}) = \sum_{j=0}^{\infty}(2j+1)^{-1}S_j P_j(\boldsymbol{u}\cdot\boldsymbol{n})$, with the scalar order parameters $S_j = \langle P_j(\boldsymbol{u}\cdot\boldsymbol{n})\rangle$, and P_j are Legendre polynomials. The S_j are bounded, $0 \leqslant S_1 \leqslant 1$ and $-1/2 \leqslant S_j \leqslant 1$ for $j > 1$. In the equilibrium state, $\boldsymbol{n}$ coincides with the unit vector of the magnetic field direction. Moreover, the orientational order parameters can be calculated explicitly as a function of the magnetic field, while satisfying the recursion relation $S_{j+1}^{\text{eq}}(h) = S_{j-1}^{\text{eq}}(h) - (2j+1)S_j^{\text{eq}}(h)/h$ with $S_0^{\text{eq}} = 1$ and $S_1^{\text{eq}}(h)$ is identical to the Langevin function $L(h)$. For spherical particles, we have shown in [11] that the assumption of uniaxial symmetry leads to very accurate results also out of equilibrium, even if the actual distribution function is not strictly uniaxial symmetric. The validity of the assumption of uniaxial symmetry for non-spherical particles is discussed in the next section. It should be noted that the so-called effective field approximation [12] assumes a special subset of uniaxially symmetric distribution functions with $S_j = S_j^{\text{eq}}(\xi_e)$, $\boldsymbol{n} = \boldsymbol{\xi}_e/\xi_e$, with $\boldsymbol{\xi}_e$ the effective field and ξ_e its norm.

Under the assumption of uniaxially symmetric distribution functions we obtain from equation (13) time evolution equations for the orientational order parameter S_1 and a balance equation for the director, see [13]:

$$\dot{S}_1 = \tfrac{3}{5}B(S_1 - S_3)(\boldsymbol{\gamma}\colon\boldsymbol{nn}) - 2D_r S_1 + \tfrac{2}{3}D_r(1-S_2)(\boldsymbol{h}\cdot\boldsymbol{n}), \tag{16}$$

$$(\mathbf{1} - \boldsymbol{nn})\cdot\left[D_r\boldsymbol{h} - \frac{3S_1}{2+S_2}\boldsymbol{N} + B\frac{3(3S_1+2S_3)}{5(2+S_2)}\boldsymbol{\gamma}\cdot\boldsymbol{n}\right] = \mathbf{0}. \tag{17}$$

Under the same assumption, the pressure tensor (8) and (9) is found to be of the form assumed in the Ericksen–Leslie theory [74, 75] and the viscosity coefficients can be identified [13]. In particular, upon inserting equation (13) into the antisymmetric stress tensor (12), we recover the Ericksen–Leslie form for $\boldsymbol{p}^{\text{a}} = \gamma_1(\boldsymbol{N}\times\boldsymbol{n}) + \gamma_2(\boldsymbol{\gamma}\cdot\boldsymbol{n})\times\boldsymbol{n}$ with the viscosity coefficients ($\Gamma \equiv 12\eta_0^{\phi}e_Q/5 = 6\eta_s\phi e_Q$)

$$\gamma_1 = \Gamma\frac{3S_1^2}{2+S_2}, \qquad \gamma_2 = -\Gamma B\frac{3S_1(3S_1+2S_3)}{5(2+S_2)}. \tag{18}$$

For spherical particles, $B = 0$, $e_Q = 1$, we recover the result obtained in [11]. Equation (18) introduces also the viscosity coefficient γ_2, which is absent in the kinetic model introduced in [12]. In the context of molecular liquids and liquid crystals, this term is known to be responsible for the flow alignment phenomenon [75, 76]. According to the result stated in equation (18), the enhancement of the rotational viscosity for non-spherical units is just given by the quantity e_Q characterizing the shape alone (see footnote 3). While $e|_{Q=1} = 1$, for an axis ratio of $Q = 10$ we predict an increase in γ_1 by about 800%. For later use, we introduce a 'tumbling parameter' $\lambda_{\text{t}} \equiv -\gamma_2/\gamma_1 = B(3S_1+2S_3)/(5S_1)$, which results from (18). From equation (16), the angle $h^{-1}\boldsymbol{h}\cdot\boldsymbol{n}$ between the direction of the magnetic field and the magnetization can also be calculated to give $h^{-1}\boldsymbol{h}\cdot\boldsymbol{n} = 3S_1h^{-1}(1-S_2)^{-1}\{1 - 3B(S_1-S_3)(5S_1)^{-1}\tau\boldsymbol{\gamma}\colon\boldsymbol{nn}\}$. The term proportional to B is responsible for the flow alignment of non-spherical particles, which is being suppressed with increasing magnetic field due to the prefactor h^{-1}.

In the weak flow regime and within the assumption of uniaxial symmetry, the order parameters S_i may be replaced by the explicitly known equilibrium values S_i^{eq} in all the above expressions. In particular, in this regime one obtains $\gamma_1^0 = \Gamma hL^2(h)/(h - L(h))$ and $\gamma_2^0 = -\Gamma BL(h)[(6+h^2)L(h) - 2h]/\{h(h - L(h))\}$. This result equals the one obtained

using the effective field approximation [12, 13]. Thus, deficiencies of the effective field approximation in the weak flow regime are due to the assumed uniaxial form of the distribution function. The effective field approximation can also be used outside the weak flow regime. The quality of this approximation had been discussed for the case of spheres ($B = 0$) in [11, 77, 79]. In [79] it is shown that the effective field approximation in the case $B = 0$ becomes exact in the limits of weak and strong magnetic fields h and that the approximation can be considered accurate for all values of h with deviations of less than 5%.

If the magnetization (and not necessarily the magnetic field) is oriented parallel to the flow, gradient and vorticity direction, the Miesowicz (shear) viscosities η_1, η_2, η_3 are measured, respectively. Using the above expressions we obtain the following results in terms of order parameters and shape coefficients:

$$\frac{\eta_1 - \eta_0}{\eta_0^\phi} = \frac{3e_Q}{5}\frac{3S_1^2}{2+S_2}(1-\lambda_t) + \left(\frac{2}{7}Q_{32} - Q_0\right)S_2 + \frac{8}{35}Q_{23}S_4, \tag{19}$$

$$\frac{\eta_2 - \eta_0}{\eta_0^\phi} = \frac{3e_Q}{5}\frac{3S_1^2}{2+S_2}(1+\lambda_t) + \left(\frac{2}{7}Q_{32} + Q_0\right)S_2 + \frac{8}{35}Q_{23}S_4, \tag{20}$$

$$\frac{\eta_3 - \eta_0}{\eta_0^\phi} = -\frac{4}{7}\left(Q_{32}S_2 + \frac{1}{10}Q_{23}S_4\right), \tag{21}$$

where the shape coefficients e_Q, B, Q_i are tabulated below (see footnote 3). As noted in section 2 a fourth viscosity coefficient η_{12} has been introduced in order to fully characterize the shear viscosity, which becomes $\eta_{12} = \alpha_1 = -2\eta_0^\phi Q_{23}S_4$, The difference between the first two Miesowicz viscosities is found to be given by

$$\frac{\eta_2 - \eta_1}{\eta_0^\phi} = \frac{6e_Q}{5}\frac{3S_1^2}{2+S_2}\lambda_t + 2Q_0S_2. \tag{22}$$

A discussion on the validity of Parodi's relation, which implies $\eta_1 - \eta_2 = \gamma_2$, can be found in [13]. The McTague viscosities are obtained from the Miesowicz viscosities through relations given in section 2. Dilute suspensions of non-spherical particles also show normal stress effects, which have been derived within the present framework in [13].

From equations (19)–(21) the effect of the shape of ellipsoids on the Miesowicz viscosities for the case of weak shear flow and under the assumption of uniaxial symmetry, where $\forall_i S_i = S_i^{\mathrm{eq}}$ is approximately valid, is immediately explored. Examples are shown in figures 2 and 3. The case of a perfectly aligned model MR fluid to be studied by simulation in section 5 corresponds to $\forall_i S_i = 1$.

4. Nonequilibrium Brownian dynamics (NEBD) simulation

In order to discuss the validity of the assumptions made in the previous sections, we here present simulation results of the numerical solution of the full kinetic model (7). The numerical solution is obtained by Brownian dynamics (BD) simulations of the stochastic process $\boldsymbol{U}_t$ that satisfy the following stochastic differential equation corresponding to the kinetic equation [80]:

$$\mathrm{d}\boldsymbol{U}_t = \boldsymbol{P}_t \cdot [(\boldsymbol{\omega} \times \boldsymbol{U}_t + B\boldsymbol{\gamma} \cdot \boldsymbol{U}_t + \boldsymbol{h})\,\mathrm{d}t + \mathrm{d}\boldsymbol{W}_t] - \boldsymbol{U}_t\frac{\mathrm{d}t}{\tau}, \tag{23}$$

The projector perpendicular to $\boldsymbol{U}_t$ is denoted by $\boldsymbol{P}_t \equiv (\mathbf{1} - \boldsymbol{U}_t\boldsymbol{U}_t)$ and $\boldsymbol{W}_t$ is a three-dimensional Wiener process [80]. Using Itô's formula, it is verified that equation (23) conserves the normalization of $\boldsymbol{U}_t$. In order to integrate equation (23) numerically, a weak first-order scheme is used. By construction, the numerical scheme guarantees the normalization of the random

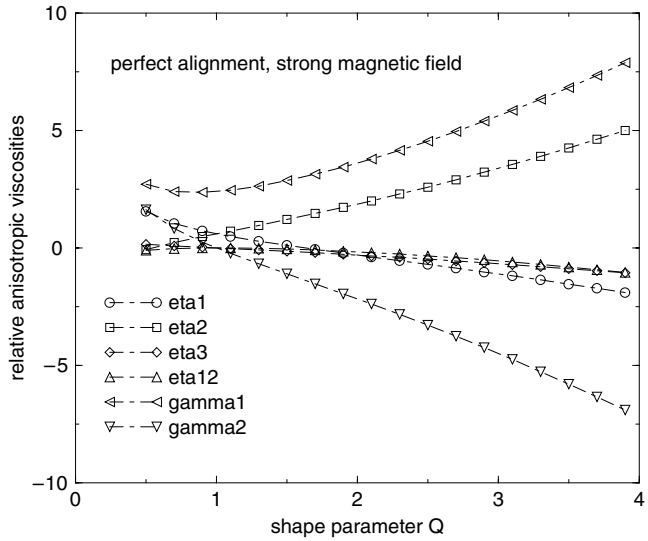

Figure 2. Miesowicz and rotational viscosities $(\eta_{1,2,3} - \eta_0)/\eta_0^\phi$, η_{12}/η_0^ϕ and $\gamma_{1,2}/\eta_0^\phi$ according to equations (18)–(21)—valid at low concentrations—versus shape coefficient Q, cf figure 1, and evaluated for the case where the strong magnetic field dominates, i.e. the order parameters are set to $\forall_i S_i = 1$. Notice that the viscosities η_0 and $\eta_0^\phi \equiv \eta_0 - \eta_s$ depend on the shape Q via equation (15), where η_s denotes the viscosity of the solvent, and expressions for the geometric coefficients $Q_{1,2,3}$ (see footnote 3), etc, appear in (15). In order to eliminate η_0, differences between the relative viscosities may be favoured to compare with experiment.

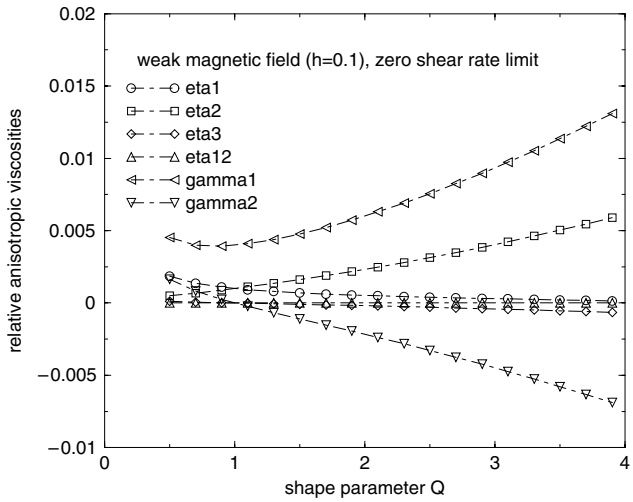

Figure 3. Same quantities as for figure 2 but for the case of weak shear flow, i.e. order parameters are set to their equilibrium values $\forall S_i = S_i^{\mathrm{eq}}(h)$ with $h = 0.1$. An explicit recursion relation for S_i^{eq} is given in section 3.2.

unit vector $\boldsymbol{U}_t$ [80]. A slightly different approach has been used to study cluster structures and magnetic characteristics of ferromagnetic particles in [81, 82]. For various initial conditions, the simulations are performed for an ensemble of 10^5 random unit vectors $\boldsymbol{U}_t$ with time step

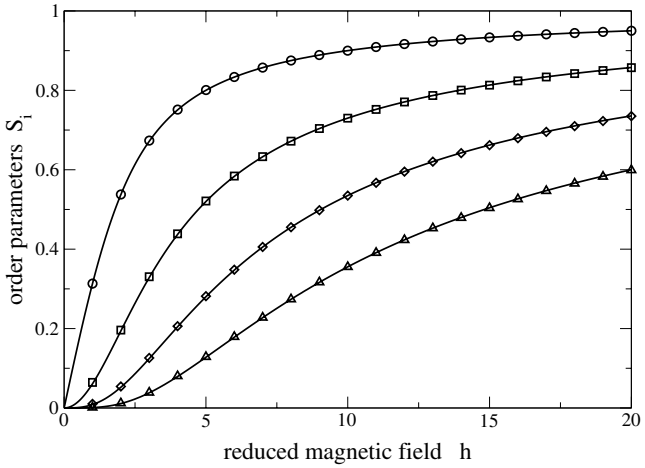

Figure 4. Orientational order parameters S_i as a function of reduced magnetic field h for plane Couette flow $\boldsymbol{v} = (\dot{\gamma} y, 0, 0)$ and magnetic field oriented in the y direction. The Péclet number is $P\acute{e} = \dot{\gamma}\tau = 0.1$ and the axis ratio was chosen as $Q = 5$. Full curves correspond to the equilibrium values S_i^{eq}, while symbols are obtained from the BD simulations using $\langle \boldsymbol{u} \rangle = S_1 \boldsymbol{n}$. The ordering of the curves from top to bottom is $i = 1, 2, 3, 4$.

$10^{-3}\tau$. Plane Couette flow is considered in order to allow comparison to the analytical results discussed above. In figure 4, the equilibrium order parameters $S_j^{\mathrm{eq}}(h)$ are shown together with those obtained from the BD simulations for a weak shear rate and magnetic field oriented in the gradient direction of the flow. From the BD simulations, S_1 and the director $\boldsymbol{n}$ are defined by $\langle \boldsymbol{u} \rangle = S_1 \boldsymbol{n}$, while higher-order parameters are obtained by suitable contractions of $\boldsymbol{n}$ with moments $\langle \boldsymbol{uu} \rangle$, $\langle \boldsymbol{uuu} \rangle$ and $\langle \boldsymbol{uuuu} \rangle$. From figure 4 we observe that S_i for $i \leqslant 4$ are very accurately described by their equilibrium values. A similar accuracy is obtained if the equilibrium value $\boldsymbol{n} = \boldsymbol{h}/h$ is chosen. Figure 5 shows the results of the BD simulations for the shear viscosities in comparison to the results in section 3.2 based on the assumption of uniaxial symmetry, where the values of the director components and the order parameters were extracted from the BD simulation. It is seen from figure 5 that the results of section 3.2 agree qualitatively with the numerical simulations. The assumption of uniaxial symmetry is violated for weak magnetic fields so that results of section 3.2 represent approximations to the actual viscosities, see the schematic diagram in figure 6 which summarizes the findings.

There have been a number of interesting simulation studies of field-induced rheology, see [83, 84] for 3D BD studies in steady shear including a phase diagram in λ, $\dot{\gamma}$ space, and [85] and [41] for 2D athermal Stokesian dynamics simulations with a highly accurate treatment of hydrodynamic and electrostatic interactions (but only 25 particles) in steady and oscillatory shear, respectively.

5. Nonequilibrium molecular dynamics (NEMD) simulation

In a molecular dynamics (MD) computer simulation for a substance composed of N particles, Newton's equations of motion are integrated numerically. Periodic boundary conditions and the nearest image convention are used in order to minimize surface effects. For particles with rotational degrees of freedom also, equations of motion for angle variables, involving the torque acting on particles, have to be solved. The temperature T of the system is linked

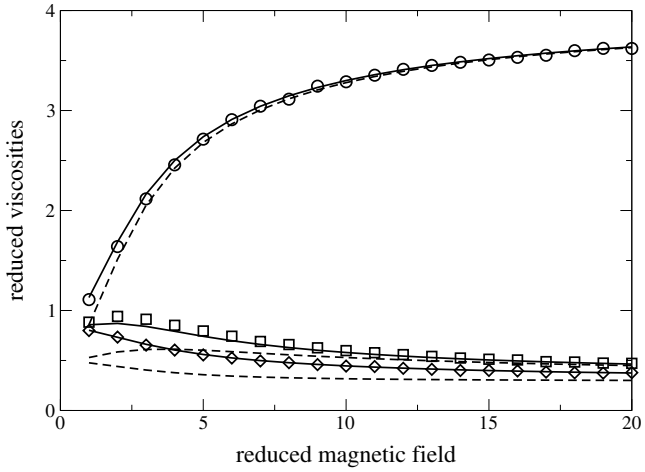

Figure 5. Viscosity change $p_{yx}/\dot{\gamma} - \eta_s$ as a function of reduced magnetic field h for plane Couette flow $\boldsymbol{v} = (\dot{\gamma} y, 0, 0)$. The Péclet number is $Pé = \dot{\gamma}\tau = 0.1$ and the axis ratio was chosen as $Q = 5$. The ordering of the curves from top to bottom corresponds to magnetic fields parallel to the velocity gradient, the velocity and the vorticity directions, respectively. Symbols denote results from BD simulation, while the full and broken lines represent the semi-analytical results of section 3 where the values for the order parameters and director components were obtained from the BD simulation.

with the part of the kinetic energy K which is not associated with a macroscopic motion: $3(N-1)k_BT/2 = K \equiv \sum_i m(c^i)^2/2$, where c^i is the translational 'peculiar velocity'. The simplest version of a 'thermostat', also used here, involves rescaling the peculiar velocity after each time step by the factor $(T_{\text{wanted}}/T_{\text{measured}})^{1/2}$. Other thermostats, e.g. those referred to as 'Gaussian' and 'Nosé-Hoover' [86], may also be imposed as constraints. The observables of interest, such as the internal energy and the components of the pressure or the stress tensor, are calculated from the known positions and velocities of the particles as time averages according to the rules of statistical physics. Similarly, more detailed information can be obtained from the simulation, such as the velocity distribution function, the pair correlation function or the static structure factor, which can also be measured in scattering experiments [27]. Dimensionless or 'scaled' variables are used which are denoted by the same symbols as the physical variables when no danger of confusion exists. For a system of spherical particles whose forces are derived from Lennard-Jones (LJ) potential Φ, depending on the distance r: $\Phi = \Phi^{LJ} \equiv 4\Phi_0[(r_0/r)^{12} - (r_0/r)^6]$, lengths and energies are presented in units of the diameter r_0 and the potential depth Φ_0. The units used for the particle density and temperature are r_0^{-3} and $k_B^{-1}\Phi_0$. The time is scaled with the reference time $t_0 = r_0 m^{1/2}\Phi_0^{-1/2}$, where m is the mass of a particle. The pressure, the shear rate and the viscosity of the LJ fluid are expressed in units of $r_0^{-3}\Phi_0$, t_0^{-1} and $r_0^{-3}\Phi_0 t_0 = r_0^{-2} m^{1/2}\Phi_0^{1/2}$. In the simulations, the cut-off of the interaction at a finite distance r_{cut} is often achieved just by putting the potential and the force equal to zero for $r > r_{\text{cut}}$, e.g. with $r_{\text{cut}} = 2.5r_0$. When only the repulsive r^{-12} part of the LJ interaction potential is taken into account, one speaks of a 'soft sphere' (ss) potential. Often, this potential is written as $\Phi = \Phi_0^{ss}(r_0/r)^{12}$ without the factor of 4 of the LJ potential. When reduced ss-units with Φ_0^{ss} as energy reference are used, $T = 1/4$ in ss-units is equivalent to $T = 1$ in LJ-units. Results to be reported in section 5 have been obtained for this particular temperature $T = 1/4$.

A simple shear flow in the x direction with the gradient in the y direction can be generated either by moving boundaries or forces [87–89], or as implemented here, by moving image

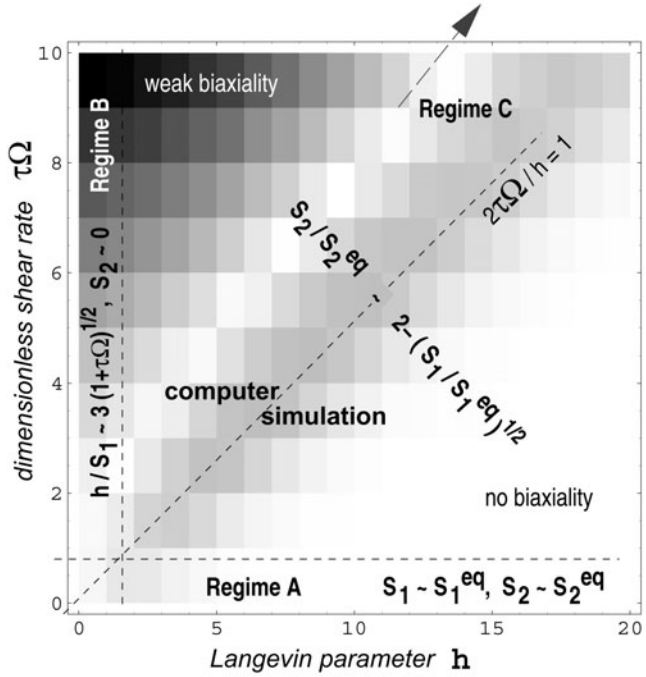

Figure 6. The shaded background represents a measure for the (minor) relevance of biaxiality—obtained via BD—on the prediction of rotational viscosity γ_1 as a function of dimensionless magnetic field h and vorticity $\tau\dot{\gamma}$ [11]. Shading ranges from white (uniaxial) to black. In the top left corner (data for $\tau\dot{\gamma} = 10$, $h = 1$) we have a 1.2% relative deviation between uniaxial (18) and biaxial formulae [11] for γ_1. The depicted regimes refer to analytical solutions of the FP equation. A: weak magnetic field, B: weak flow field, C: deterministic limit, discussed in section 3. The figure summarizes analytical as well as approximate results for these regimes.

particles undergoing an ideal Couette flow with the prescribed shear rate $\dot{\gamma} = \partial v_x/\partial y$ (homogeneous shear). For details on the realization of a NEMD shear flow we wish to refer to the reviews [27, 28] and references cited herein.

6. Magneto-rheological fluids via NEMD

6.1. Perfectly aligned moments

The model studied here deals with a relatively dense solution of a MR fluid, or alternatively, a ferrofluid subject to large external magnetic field. The particles occupy 10% or more of the available volume. It is assumed that the applied magnetic field is strong enough, such that all magnetic moments are perfectly parallel to the external field. In addition to a repulsive isotropic interaction, the angle dependence of the dipole–dipole interaction is taken into account. For computational simplicity, the interaction is cut off at a finite distance. Thus effects associated with the long-range character of the dipole–dipole interaction are disregarded within this model. However, they can be taken into account by considering Ewald summations or a reaction field as described in [90]. Furthermore, it is assumed that the dynamics is dominated by the particle–particle interaction, the background fluid (solvent) enters only via the local thermostat which removes the heat generated in a viscous flow. Of course, additional friction forces and fluctuating forces due to the solvent can and have been taken into account [41, 85, 91].

Table 1. The (potential contributions to the) Miesowicz viscosities $\eta_{1,2,3}$, the Helfrich viscosity η_{12}, the Leslie viscosities $\gamma_{1,2}$ and the coupling coefficient κ of the SSD ferrofluid at $n = 0.6$, for $\lambda = 0.8$. The data are inferred from the NEMD simulations [30], in the limit of small shear rates.

Model	η_1	η_2	η_3	η_{12}	γ_1	γ_2	κ
SSD	0.63(5)	0.43(4)	0.50(5)	2.0(1)	0.16(2)	0.17(2)	0.6(1)

Spherical colloidal particles with a magnetic core as they occur in ferrofluids in the presence of an applied magnetic field parallel to the unit vector $\boldsymbol{n}$, have been modelled by soft spheres plus a dipole–dipole interaction (SSD) [92]:

$$\Phi = \Phi_0^{\mathrm{ss}}\left[\left(\frac{r_0}{r}\right)^{12} - \lambda\left(\frac{r_0}{r}\right)^{3}(3r^{-2}(\boldsymbol{r}\cdot\boldsymbol{n})^2 - 1)\right]. \tag{24}$$

The parameter $\lambda > 0$ is proportional to the square of the (induced) magnetic moments of the particles which are parallel to $\boldsymbol{n}$, i.e. $\lambda = \mu^2/T$ in reduced simulation units. The quantities r_0 and Φ_0^{ss} set the length and energy scales.

6.2. Viscosity coefficients

Pairs of particles feel a disc-like interaction (corresponding to $r < 1$, $B < 0$) since, for fixed relative kinetic energy, they can approach each other more closely in the direction parallel to $\boldsymbol{n}$ rather than in the perpendicular directions. Thus it is not surprising that ferrofluids subject to strong magnetic fields, but small λ compared to that of a typical MR fluid, show an anisotropy analogous to nematic discotic liquid crystals [1, 93]. In table 1, NEMD results are presented for the only state point where all viscosities (except the bulk viscosity) have been determined.

When the dipole–dipole interaction is stronger (the regime of MR fluids), however, chains are formed which, at higher densities, are arranged in partially ordered spatial structures. This affects the viscous behaviour in a dramatic way. An example is shown in figure 7 where the viscosities η_1 (magnetic field parallel to the flow velocity) and η_2 (magnetic field parallel to the gradient of the flow velocity) are plotted as functions of the anisotropy (or magnetic interaction) parameter λ. The state point is $n = 0.6$ in soft sphere units and the shear rate is $\dot{\gamma} = 0.06$ (and $T = 1/4$, of course). The interaction is cut-off at $r_{\mathrm{cut}} = 2.5r_0$, and $(r_0/r)^3$ in (24) is replaced by $(r_0/r)^3 - (r_0/r_{\mathrm{cut}})^3 + 3(r_0/r_{\mathrm{cut}})^4(r/r_0 - r_{\mathrm{cut}}/r_0)$ in order to achieve a smoother cut-off. The simulations were made with $N = 1000$ particles [94]. For $0 < \lambda < 1$, the discotic behaviour $\eta_1 > \eta_2$ is seen in figure 7. For $\lambda > 1$, the viscosity η_2 for the field parallel to the gradient direction increases strongly with increasing λ. Notice that a logarithmic scale is used for the viscosity.

The viscosities and the shear-induced structural changes were analysed in orientations 1 and 2 for number densities between $n = 0.2$ and 0.8, corresponding to packing fractions of about 0.1–0.4, and for the magnetic interaction strength λ ranging from 0 to 8/3. Figure 8 shows results for a specific case of interest. Breaking and reformation of chains and of more complex structures, under shear flow, have been observed.

Model predictions for the Miesowicz viscosities based on the measured shape of agglomerates Q versus dimensionless magnetic moment μ, or $\sqrt{\lambda}/2$ in terms of the interaction parameter λ, are shown in figure 9. The data for Q and $\eta_{1,2}$ are obtained from NVT MD simulation (reduced shear rate $\dot{\gamma} = 0.1$, packing fraction $\phi = 0.31$). Here, the shape Q is obtained from the locations of the first relative minimum of the structure factor at low wavevector transfer, when evaluated parallel and perpendicular to the magnetization, respectively, i.e. $r = q_\perp/q_\parallel$.

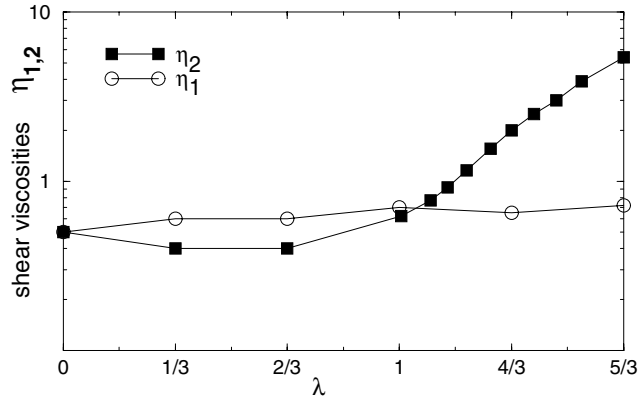

Figure 7. The viscosity coefficients η_1, η_2 plotted as a function of the strength λ of the dipole–dipole interaction for $\phi = 0.31$ and $\dot{\gamma} = 0.06$ in soft sphere units (data obtained via MD).

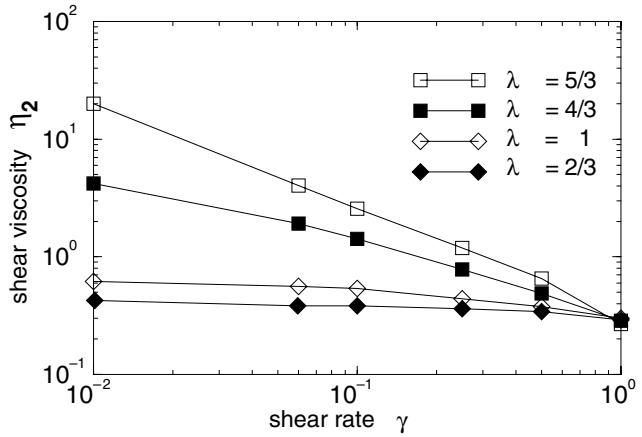

Figure 8. The effect of λ on the potential contribution to the shear viscosity η_2 versus shear rate $\dot{\gamma}$ in soft sphere units. Data obtained from MD, cf figure 7.

The microstructure and its relation to the magnetic properties of ferrofluids are often investigated by performing a cluster analysis. In conventional cluster analysis, agglomerates are usually defined on the base of the spatial proximity between the particles or by means of an energy criterion. For ferrofluids the latter one is more favourable, because the anisotropic dipolar interaction implies that two neighbouring particles can form a stable bonding only if their dipole moments are roughly aligned in head-to-tail orientation. The energetically based cluster analysis of ferrofluids has been done in several different ways [22, 95–99]. In [22, 95–97] two particles are considered to be bound if their dipolar potential energy is less than a predetermined value. The influence of using different threshold values for this value had been investigated in [100]. The rather simple definition based on the structure factor is based on the fact that ellipsoidal shaped particles with homogeneous scattering density yield ellipsoidal shaped structure factors as long as the packing fraction is low and spatial correlations between clusters are negligible.

In figure 9—for comparison—the predictions of the affine transformation model [101] $\eta_1 = \eta_{\mathrm{iso}} Q^{-2}$, $\eta_2 = \eta_{\mathrm{iso}} Q^2$, see also figure 10, and the results presented in section 3

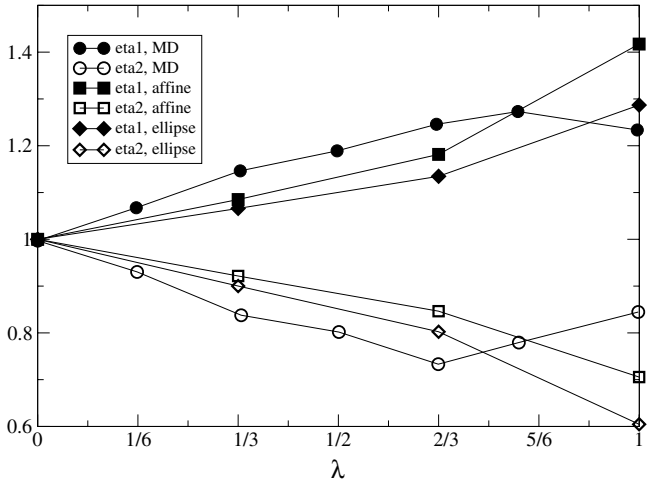

Figure 9. Model predictions for the Miesowicz viscosities $\eta_{1,2}$ based on the measured shape of agglomerates Q versus magnetic interaction parameter λ. Data for Q and $\eta_{1,2}$ are taken from [30], where Q is obtained from the anisotropy of the structure factor at low wavevector transfer in a NVT MD simulation (500 particles, reduced temperature $T = 1/4$, reduced shear rate $\dot{\gamma} = 0.1$, packing faction $\phi = 0.31$). For comparison, the predictions of the affine transformation model [101] and the results presented in section 3 for ellipses are included in this plot.

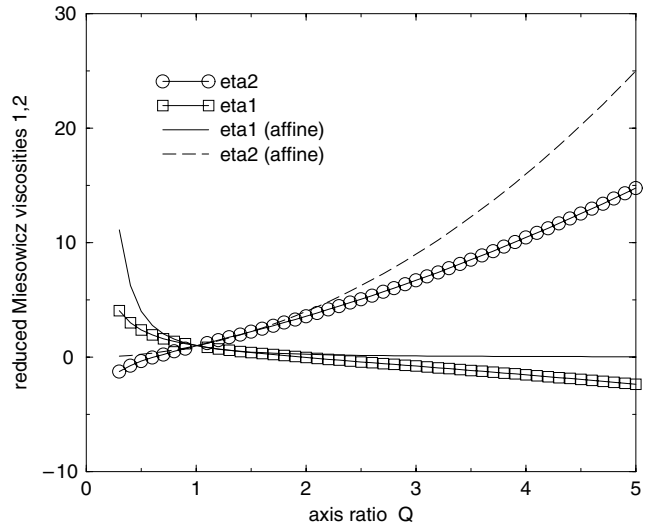

Figure 10. Comparison between the predictions for reduced Miesowicz viscosities $\eta_{1,2}$ (here $\eta_{1,2} = 1$ for spheres, i.e. $Q = 1$) for the two models discussed in figure 9 versus axis ratio Q of ellipsoids of revolution. Notice that $\eta_1 < \eta_2$ and $\eta_1 > \eta_2$ is predicted from both models for $Q > 1$ (prolate) and $Q < 1$ (oblate ellipsoids), respectively.

are included. The two latter models assume a low packing fraction and do not consider dipolar interaction between particles, and therefore deviate from the MD results. In linear order $Q = 1 + \epsilon$ the affine transformation model yields $(\eta_{2/1} - \eta_{\rm iso})/\eta_{\rm iso} = 1 \pm 2\epsilon$ and $(\eta_1 - \eta_2)/\eta_{\rm iso} = -4\epsilon$, while our equation (19) yields $(\eta_1 - \eta_1|_{Q=1})/(\eta_1|_{Q=1} - \eta_s) = 1 - 41/70\epsilon$, $(\eta_2 - \eta_2|_{Q=1})/(\eta_2|_{Q=1} - \eta_s) = 1 + 32/35\epsilon$, where η_s denotes the viscosity of the solvent.

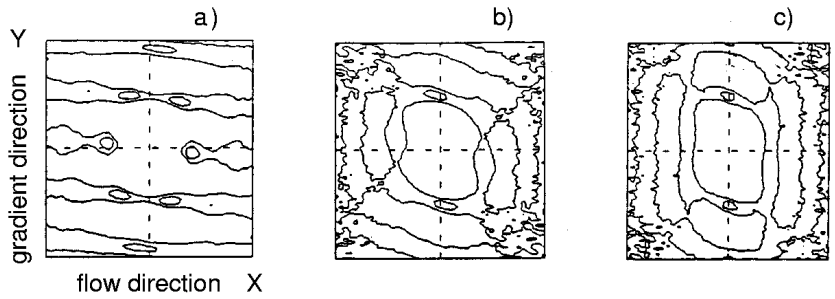

Figure 11. Effect of shear rate on the static structure factor ($\phi = 0.31$, magnetic field in the y direction, see figure 1, magnetic interaction strength $\lambda = 2$), contour-projected onto the shearing plane, extracted from NEMD particle configurations for three shear rates $\dot{\gamma} = 0.01$ (a), $\dot{\gamma} = 0.5$ (b) and $\dot{\gamma} = 1$ (c).

A yield stress occurs for the higher values of the dipole–dipole interaction. This is typical for the MR fluids, which are similar to the ferrofluids under a strong magnetic field, but which are composed of particles with stronger dipole–dipole interactions and usually contain a higher volume fraction of colloidal particles. ER fluids can, with appropriate modifications, also be treated theoretically by the model. For simulations where solvent effects and hydrodynamic interactions are also taken into account, see [91]. The transition from the ferrofluid to the magneto-rheological behaviour, with increasing magnetic interaction, is analogous to what one might expect in a nematic discotic system which can undergo a transition to a columnar phase at lower temperatures.

6.3. Shear thinning and shear-induced structural changes

The chains formed in MR fluids break and are reformed under shear. The viscosity becomes smaller with increasing shear rate: shear thinning [81, 82]. In figure 8, the viscosity η_2, namely with the magnetic field parallel to the gradient direction, is plotted as a function of the shear rate for various values of the parameter λ determining the strength of the dipole–dipole interaction. The behaviour seen is typical for MR fluids.

Structural changes associated with this behaviour can and have been analysed in the simulations by inspecting snapshots of particle positions by computing (partial) pair-correlation functions and the anisotropy of the static structure factor. The latter quantity can be measured, for example, in neutron scattering experiments [46]. An example for the influence of an increasing shear rate on the structure factor is shown in figure 11.

Ferrofluids composed of particles with strong permanent dipole moments and sufficiently high concentration form wormlike chains even when no magnetic field is applied [102]. The agglomerates can break by thermal agitation, and even more so, when subjected to a shear flow. This leads to a pronounced shear thinning behaviour, analogous to that seen in NEMD computer simulation studies of wormlike micellar systems, cf [32]. Given the strength of the 'binding energy' or 'scission energy' E_{sc} between neighbours in a linear chain, the dependence of the average (dimensionless) chain length, which may also be considered as the axis ratio of an ellipsoid, Q, on the shear rate, can be computed [33]. For an alternative approach, the 'chain model of electrorheology', which also predicts shear-induced lifetimes of chains, we refer the interested reader to [103]. In equilibrium, one expects—for stiff linear chains—a simple exponential increase of the number averaged length with E_{sc} and a square root increase with concentration, i.e. $Q \propto \phi^{1/2} \exp(E_{sc}/2k_BT)$. For the MR system under

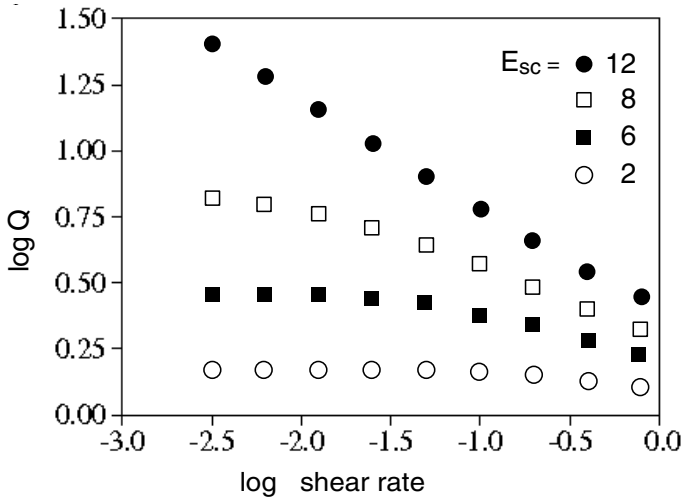

Figure 12. Analytically predicted effect of shear rate on the average length $\bar{L}$ for a wormlike micellar solution ($\phi = 0.04$) parametrized in the scission energy E_{sc} [33]. A relationship between the scission energy E_{sc} and the magnetic interaction parameter behaviour of MR fluids and wormlike micellar solutions is established in the text.

consideration, the scission energy may be roughly estimated from the energy minimum in (24), with $\boldsymbol{r} \parallel \boldsymbol{n}$, i.e. $E_{sc} = \Phi_0 \lambda^{4/3}(3/2)2^{-1/3}$. We therefore expect for the number average $Q \propto \phi^{1/2} \exp(3\lambda^{4/3}2^{-1/3})$ and a monoexponential distribution of lengths, at low concentrations. Corrections for higher concentrations and the effect of semiflexibility (persistence length) and ring formation on the shape of agglomerates has been discussed, for example, in [104]. The effect of alignment and stretching of transient chains on their length distribution, the shear viscosity and normal stresses in the (magnetic) field-free case has been estimated in the framework of a modified Rouse model [33]: a sample result is reproduced in figure 12.

Due to the stretching and alignment, shear thinning is also observed when chains do not break. From the computer simulations we infer that the shear rate dependence of the normal stress differences is a more sensitive indicator of the breaking of chains. Thus measurements of at least the first normal pressure difference of ferrofluids are of interest.

7. Conclusions

Some recent works on the rheology, dynamics and structure of ferrofluids and MR fluids have been summarized and compared to each other. The FP equation discussed in this paper provides a robust starting point for the description of the properties of dilute suspensions. By solving the FP equation numerically (via BD simulation) the assumption of orientational uniaxiality has been supported, namely figure 6. Using this assumption the complete set of anisotropic viscosities has been expressed in terms of order parameters characterizing the uniaxial phase, packing fraction and solvent viscosity. The magnetization is expressed in terms of the first order parameter, and expressions for the equilibrium and stationary order parameters have been obtained analytically as well as numerically. Dynamical equations for the order parameters have also been given. While the FP equation incorporates the rotation of individual moments caused by the vorticity of the flow field, and deformation or pseudoaffine motion of nonspherical objects, within a MD (more microscopic) simulation one is confronted

with the description of the coupling between flow and rotation of suspended particles due to friction, and the effect of hydrodynamic screening within clusters of particles. In order to prevent any ambiguities in the modelling approach, we presented results for an idealized isothermal many-particle model of perfectly oriented magnetic moments (in the bulk), which interact through soft-sphere repulsion and dipolar interaction. This model provides results in qualitative agreement with experimental findings for ferrofluids subject to strong magnetic fields and MR fluids. A sign change in the rotational viscosity γ_2 upon increasing the magnetic interaction parameter is predicted and now qualitatively understood. The calculation of the effect of packing fraction on the rheological and structural behaviour still offers a number of challenging aspects. The precise intermolecular potentials between ferromagnetic particles are still unknown (and different for different coatings), and the size and shape of agglomerates, and their dynamics, can be expected to be strongly depended on the form of these potentials.

Acknowledgments

Financial support by the Deutsche Forschungsgemeinschaft through the priority program 'Kolloidale magnetische Flüssigkeiten' is gratefully acknowledged.

Note added in proof. An adjudicator motivated us to supplement this paper with the following discussion.

The referee expresses strong doubts about the validity of the expression for the antisymmetric, hydrodynamic stress tensor, see equation (9). He/she states: 'Here the hydrodynamic contribution corresponding to rotational friction is missing. The term given in equation (9) is the antisymmetric part of the Maxwell pressure tensor. In the steady state both should cancel, see the discussion in [57]. The equation is inconsistent with equation (8), where the hydrodynamic contribution to the symmetric part of the pressure tensor is taken into account. The fact that antisymmetric stress is treated incorrectly in many publications is no argument for repeating the error. It has been shown by Felderhof, see [105], how magnetoviscosity comes about, even with a symmetric pressure tensor'.

Reference [105] is the more recent of the two references mentioned and abbreviated as 'reference A' in the following. We should state why we consider, through equations (8) and (9), the hydrodynamic (part of the) pressure tensor, which is the negative of the hydrodynamic stress tensor. In this paper we make a comparison with the Ericksen–Leslie theory for the *hydrodynamic* stress, by which the viscosity coefficients are actually defined. According to equation (1) the antisymmetric part of the *pressure* tensor is $(1/2)\boldsymbol{\epsilon}\cdot\boldsymbol{p}^{\mathrm{a}}$. with $\boldsymbol{p}^{\mathrm{a}} = -n\langle\boldsymbol{\mathcal{L}}V\rangle$, cf our equation (8). The potential $V = -\mu\boldsymbol{H}\cdot\boldsymbol{u}$ and magnetization $\boldsymbol{M} = n\mu\langle\boldsymbol{u}\rangle$ are defined after equation (7). We therefore have $\boldsymbol{p}^{\mathrm{a}} = \boldsymbol{M}\times\boldsymbol{H}$, which is (now) explicitly stated in equation (11). Combining equations (3.2) of reference A—which implies $\boldsymbol{p}^{\mathrm{a}} = -4\zeta\{\boldsymbol{\omega}-\tilde{\boldsymbol{\omega}}\}$, $\boldsymbol{\omega}\equiv(\nabla\times\boldsymbol{v})/2$—with equation (2.14) of the reference A—which gives $\tilde{\boldsymbol{\omega}} = \boldsymbol{\omega} + (\boldsymbol{M}\times\boldsymbol{H})/(4\zeta)$, we just reobtains our equations (9) and (11). The hydrodynamic part corresponding to rotational friction should therefore be present. The FP approach considered in this paper naturally disregards magnetization inertia effects, which are usually small, and 'may be neglected', as pointed out after equation (2.13) of reference A.

References

[1] Hess S 1986 *J. Non-Equilib. Thermodyn.* **11** 175
[2] Miesowicz M 1935 *Nature* **17** 261
Miesowicz M 1946 *Nature* **158** 27
[3] Ericksen J L 1960 *Arch. Ration. Mech. Anal.* **4** 231
Ericksen J L 1969 *Mol. Cryst. Liq. Cryst.* **7** 153
Leslie F M 1966 *J. Mech. Appl. Math.* **19** 357
Leslie F M 1968 *Arch. Ration. Mech. Anal.* **28** 265
[4] Parodi O 1970 *J. Physique* **31** 581
[5] de Gennes P G 1974 *The Physics of Liquid Crystals* (Oxford: Clarendon) ch 3
[6] Kelker H and Hatz R 1980 *Handbook of Liquid Crystals* (Weinheim: Verlag Chemie)
[7] Vertogen G and deJeu W 1988 Thermotropic liquid crystals, fundamentals *Chemical Physics* vol 45 (Berlin: Springer)
[8] Shliomis M I 1972 *Sov. Phys.–JETP* **34** 1291
[9] Hall W F and Busenberg S N 1969 *J. Chem. Phys.* **51** 137

[10] Coffey W T and Fannin P C 2002 *J. Phys.: Condens. Matter* **14** 3677
[11] Ilg P, Kröger M and Hess S 2002 *J. Chem. Phys.* **116** 9078
[12] Martsenyuk M A, Raikher Yu L and Shliomis M I 1974 *Sov. Phys.–JETP* **38** 413
[13] Ilg P and Kröger M 2002 *Phys. Rev.* E **66** 021501
[14] Onsager L J 1936 *J. Am. Chem. Soc.* **58** 1486
[15] O'Grady K *et al* 1983 *J. Magn. Magn. Mater.* **31–34** 958
[16] Wertheim M S 1971 *J. Chem. Phys.* **55** 4291
[17] Morozov K I and Lebedev A V 1990 *J. Magn. Magn. Mater.* **85** 51
[18] Buyevich Y A and Ivanov A O 1992 *Physica* A **190** 276
[19] Pshenichnikov A F, Mekhonoshin V V and Lebedev A V 1996 *J. Magn. Magn. Mater.* **161** 94
[20] Ivanov A O and Kuznetsova O B 2001 *Phys. Rev.* E **64** 041405
[21] Huke B and Lücke M 2000 *Phys. Rev.* E **62** 6875
[22] Wang Z, Holm C and Müller H W 2002 *Phys. Rev.* E **66** 021405
[23] Ilg P and Hess S 2002 Effect of dipolar interactions on the magnetoviscosity of ferrofluids: a dynamic mean field study *Preprint*
[24] Hess S 1976 *Z. Naturf.* A **31** 1034
[25] Hess S, Hayter J B and Pynn R 1984 *Mol. Phys.* **53** 1527
Hess S 1987 Structure and dynamics of oriented ferrofluids *Physics of Complex and Supermolecular Fluids* ed S A Safran and N A Clark (New York: Wiley) p 631
[26] Hess S, Schwarzl J F and Baalss D 1990 *J. Phys.: Condens. Matter* **2** SA279
[27] Hess S, Kröger M, Loose W, Pereira Borgmeyer C, Schramek R, Voigt H and Weider T 1996 Simple and complex fluids under shear *Monte Carlo and Molecular Dynamics of Condensed Matter Systems (IPS Conf. Proc. vol 49 (Bologna, 1996))* ed K Binder and G Ciccotti pp 825–41
[28] Hess S, Aust C, Bennett L, Kröger M, Pereira Borgmeyer C and Weider T 1997 *Physica* A **240** 126
Hess S 2000 Flow properties and structure of anisotropic fluids studied by non-equilibrium molecular dynamics and flow properties of other complex fluids: polymeric liquids, ferro-fluids and magneto-rheological fluids *Advances in the Computer Simulation of Liquid Crystals* ed P Parisi and C Zannoni (Dordrecht: Kluwer)
[29] Hess S and Weider T 1996 Flow properties and structural changes in magneto-rheological fluids via non-equilibrium molecular dynamics *Proc. 12th Int. Congr. Rheol.* ed A Ait-Kadi, J M Dealy, D F James and M C Williams (Quebec: Can. Rheol. Group) pp 313–14
[30] Hess S, Weider T and Kröger M 2001 *Magnetohydrodyn.* **37** 297
[31] Wang S-Q, Gelbart W M and Ben-Shaul A 1990 *J. Phys. Chem.* **94** 2219
[32] Kröger M and Makhloufi R 1996 *Phys. Rev.* E **53** 2531
[33] Carl W, Makhloufi R and Kröger M 1997 *J. Physique* II **7** 931
[34] Kröger M 2003 Simple models for complex fluids *Phys. Rep.* at press
[35] Rosensweig R E 1985 *Ferrohydrodynamics* (Cambridge: Cambridge University Press)
[36] Tsvetkov V N 1939 *Acta. Phys. Chim. USSR* **10** 555
[37] Gasparoux H and Prost J 1971 *J. Physique* **32** 953
Prost J and Gasparoux H 1971 *Phys. Lett.* A **36** 245
[38] Heppke G and Schneider F 1972 *Z. Naturf.* A **27** 976
Heppke G and Schneider F 1973 *Z. Naturf.* A **28** 994
[39] McTague J P 1969 *J. Chem. Phys.* **51** 133
[40] Odenbach S 2000 *Int. J. Mod. Phys.* B **14** 1615
Odenbach S 1993 *Adv. Colloid Interface Sci.* **46** 263
[41] Rankin P J, Ginder J M and Klingenberg D J 1998 *Curr. Opin. Colloid Interface Sci.* **3** 373
[42] Odenbach S 2000 *Appl. Rheol.* **10** 178
[43] Odenbach S and Störk H 1998 *J. Magn. Magn. Mater.* **183** 188
Ambacher O, Odenbach S and Stierstadt K 1992 *Z. Phys.* B **86** 29
[44] Odenbach S, Rylewicz T and Heyen M 1999 *J. Magn. Magn. Mater.* **201** 155
Odenbach S, Rylewicz T and Rath H 1999 *Phys. Fluids* **11** 10
[45] Weiss K D, Carlson J D and Nixon D A 1994 *J. Intell. Mater. Syst. Struct.* **5** 772
[46] Odenbach S, Gilly H and Lindner P 1999 *J. Magn. Magn. Mater.* **201** 353
[47] Odenbach S 1999 *J. Magn. Magn. Mater.* **201** 149
[48] Gavin H P 1997 *J. Non-Newton. Fluid Mech.* **71** 165
[49] Rosensweig R E 1995 *J. Rheol.* **39** 179
[50] Bossis G, Lemaire E and Volkova O 1997 *J. Rheol.* **41** 687
[51] Tao R 2001 *J. Phys.: Condens. Matter* **13** R979
[52] Kröger M and Sellers H S 1995 *J. Chem. Phys.* **103** 807

[53] Blums E, Cebers A and Maiorov M M 1997 *Magnetic Fluids* (Berlin: de Gruyter)
[54] Brenner H and Condiff D W 1974 *J. Colloid Interface Sci.* **47** 199
[55] Müller H W and Liu M 2001 *Phys. Rev.* E **64** 061405
[56] Jansons K M 1983 *J. Fluid Mech.* **137** 187
[57] Kroh H J and Felderhof B U 1987 *Z. Phys.* B **66** 1–6
[58] Chrzanowska A, Kröger M and Sellers S 1999 *Phys. Rev.* E **60** 4226
[59] Marrucci G 1982 *Mol. Cryst. Liq. Cryst.* **72** 153
[60] Semenov A N 1983 *Zh. Eksp. Teor. Fiz.* **85** 549
[61] N Kuzuu and Doi M 3486 *J. Phys. Soc. Japan* **52**
[62] Osipov M A and Terentjev E M 1989 *Phys. Lett.* A **134** 301
Osipov M A and Terentjev E M 1989 *Z. Naturf.* A **44** 785
[63] Terentjev E M and Osipov M A 1991 *Z. Naturf.* A **46** 733
[64] Stepanov V I 1992 *Z. Naturf.* A **47** 625
[65] Chrzanowska A and Sokalski K 1992 *Z. Naturf.* A **47** 565
[66] Das P and Schwarz W 1994 *Mol. Cryst. Liq. Cryst.* **239** 27
[67] Osipov M A, Sluckin T J and Terentjev E M 1995 *Liq. Cryst.* **19** 197
[68] Kröger M and Sellers S 1997 *Mol. Cryst. Liq. Cryst.* **293** 17
[69] Archer L A and Larson R G 1995 *J. Chem. Phys.* **103** 3108
[70] Chrzanowska A and Sokalski K 1995 *Phys. Rev.* E **52** 5228
[71] Fialkowski M 1996 *Phys. Rev.* E **53** 721
[72] Blenk S, Ehrentraut H and Muschik W 1991 *Physica* A **174** 119
[73] Blenk S and Muschik W 1991 *J. Nonequil. Thermodyn.* **16** 67
[74] Leslie F M 1968 *Arch. Ration. Mech. Anal.* **28** 256
[75] Chandrasekhar S 1992 *Liquid Crystals* 2nd edn (Cambridge: Cambridge University Press)
[76] Pereira Borgmeyer C and Hess S 1995 *J. Non-Equilib. Thermodyn.* **20** 359
[77] Martsenyuk M A 1973 *J. Appl. Mech. Tech. Phys.* **14** 564
[78] Jansons K M 1983 *J. Fluid Mech.* **137** 187
[79] Felderhof B U 2000 *Magnetohydrodynamics* **36** 396
[80] Öttinger H C 1996 *Stochastic Processes in Polymeric Fluids* (Berlin: Springer)
[81] Morimoto H 2001 *Int. J. Mod. Phys.* B **15** 823
[82] Martin J E 2001 *Mod. Phys.* B **15** 574
[83] Whittle M 1990 *J. Non-Newton. Fluid Mech.* **37** 223
[84] Melrose J R 1992 *Mol. Phys.* **76** 635
[85] Bonnecaze T R and Brady J F 1992 *J. Chem. Phys.* **96** 2183
[86] Hoover W G 1986 *Molecular Dynamics* (Berlin: Springer)
Hoover W G 1991 *Computational Statistical Mechanics* (Amsterdam: Elsevier)
[87] Ashurst W T and Hoover W G 1972 *Am. Phys. Soc.* **17** 1196
Ashurst W T and Hoover W G 1972 *Phys. Rev. Lett.* **31** 206
Ashurst W T and Hoover W G 1975 *Phys. Rev.* A **11** 658
[88] Gosling E M, McDonald I R and Singer K 1973 *Mol. Phys.* **26** 1475
[89] Hess S and Loose W 1989 *Physica* A **162** 138
[90] Allen M P and Tildesley D J 1987 *Computer Simulation of Liquids* (Oxford: Clarendon)
[91] Bossis G, Grasselli Y, Lemaire E, Meunier A, Brady J F and Phung T 1993 *Phys. Scr.* T **49** 89
[92] Hess S, Hayter J B and Pynn R 1984 *Mol. Phys.* **53** 1527
[93] Hess S, Schwarzl J and Baalss D 1990 *J. Phys.: Condens. Matter* **2** SA 279
[94] Weider T 1995 *Simulation kristalliner Strukturen unter Scherung Dissertation* (Berlin: Wissenschaft and Technik Verlag)
[95] Weis J J and Levesque D 1993 *Phys. Rev. Lett.* **71** 2729
[96] Levesque D and Weis J J 1994 *Phys. Rev.* E **49** 5131
[97] Stevens M J and Grest G S 1995 *Phys. Rev.* E **51** 5962
[98] Pshenichnikov A F and Mekhonoshin V V 2000 *J. Magn. Magn. Mater.* **213** 357
[99] Coverdale G N *et al* 1998 *J. Magn. Magn. Mater.* **188** 41
[100] Tavares J M, Weis J J and da Gama M M T 1999 *Phys. Rev.* E **59** 4388
[101] Baalss D and Hess S 1988 *Z. Naturf.* A **43** 662
[102] de Gennes P G and Pincus P 1970 *Phys. Kondens. Mater.* **11** 189
[103] Martin J E and Anderson R A 1996 *J. Chem. Phys.* **103** 4814
[104] Kröger M 1998 *Macromol. Chem. Macromol. Symp.* **133** 101
[105] Felderhof B U 2000 *Phys. Rev.* E **62** 3848